activation of *IL8*. In addition to IL8, we showed that SFPQ bound to gene promoters containing the predicted SFPQ binding motif and that SFPQ binding was reduced by poly I:C stimulation (Table S3). Next, we examined whether NEAT1 is an upstream negative regulator of SFPQ in the repression of the *IL8* gene expression. IL8 mRNA induction by SFPQ depletion was not cancelled by NEAT1 depletion (see poly I:C− condition in Figure S3J). We then examined whether the NEAT1 silencing-mediated re-repression of the IL8 gene would be cancelled by SFPQ depletion. The results showed that poly I:C-induced IL8 mRNA induction was abrogated by NEAT1 knockdown and that the NEAT1 silencing-dependent rerepression of *IL8* gene induction was cancelled by SFPQ knockdown (Figure S3J). These data support the idea in which NEAT1 plays a role as an upstream negative regulator of SFPQ in the repression of the *IL8* gene expression.

To further test our model, we generated SFPQ mutants (ΔRRM1 and ΔRRM2) that retained their ability to bind to the IL8 promoter, but were unable to bind to NEAT1v2 (Figures 4A–4C). These mutants were able to suppress the IL8 expression in response to elevated levels of mNeat1v2 (Figure 4D). Moreover, the repression activity of the mutant SFPQs was stronger than that of wild-type SFPQ (Figure 4D). Experiments using systematically constructed plasmids expressing parts of NEAT1 indicated that an approximately 15 kb portion of NEAT1 was required for IL8 mRNA induction (Figure 4E). Simultaneously, RNA immunoprecipitation (RIP) results in capturing endogenous SFPQ showed that the 15 kb portion of NEAT1 bound to SFPQ in vivo.

Since SFPQ forms a heterodimer with NONO, we examined the contribution of NONO to the function of SFPQ binding to the IL8 promoter. We found that NONO depletion reduced the binding of SFPQ to the IL8 promoter region (Figure S3K). NONO depletion did not affect the expression level of SFPQ (Figure S3L), thereby ruling out the possibility that the reduced SFPQ binding to the IL8 promoter was caused by a reduced amount of SFPQ in response to NONO depletion. These results suggest that NONO affects the binding activity of SFPQ to the IL8 promoter region. In vitro binding assays showed that SFPQ/NONO had a specific binding affinity for an IL8 promoter DNA containing the SFPQ binding motif (Figure S3M). In addition, total RNA isolated from control cells expressing excess amount of NEAT1v2 abrogated SFPQ/NONO-IL8 promoter complex, but that from control cells expressing normal amount of NEAT1 did not (Figure S3N). The destruction of SFPQ/NONO-IL8 promoter complex by total RNA isolated from the cells depleted in NEAT1 was weaker than that by total RNA from the control cells (Figure S3N).

Involvement of NEAT1 in Immune Response upon Viral Infection

We next infected culture cells with either influenza virus, herpes simplex virus 1 (HSV-1), or measles virus (MV) to examine the biological significance of our earlier observations. Influenza virus is recognized by TLR3 in host cells, leading to an immune response that includes *IL8* induction (Guillot et al., 2005). Viral-derived dsRNA produced during the HSV-1 replication cycle also triggers an immune response through TLR3 stimulation (Lafaille et al., 2012; Zhang et al., 2007). Conversely, MV infection is not sensed by TLR3 (Berghäll et al., 2006). As expected, influenza virus and HSV-1, but not MV, induced NEAT1v2 expression (Figure 5A). Corresponding with this, HSV-1 infection induced excess formation of paraspeckles without altering the levels of paraspeckle proteins (Figures 5B and 5C and Figure S5A). HSV-1 also induced NEAT1 and the excess formation of paraspeckles in immune cells (Figures S5B and S5C). As expected, MV did not cause excess formation of paraspeckles (Figures S5D and S5F). Influenza virus infection induced excess formation of paraspeckles, even though the paraspeckles were slightly diffuse (Figures S5E and S5G). The *IL8* induction by influenza virus infection was decreased by NEAT1 knockdown (Figures 5D and 5E). In addition, mice infected with influenza virus or HSV-1 induced mNeat1v2 (Figure S5H). These data suggest that the regulation and function of NEAT1 in response to virus infection is evolutionarily conserved.

Cytokines secreted from the cells in response to pathogen infections are known to induce osteoclast differentiation of mouse bone marrow cells (Koide et al., 2010), so bone marrow differentiation can be used to assess the activation of the innate immune response. We therefore carried out the ex vivo experiment using mouse bone marrow cells to get further evidence of involvement of NEAT1 in innate immune response. The supernatant of virus-infected cells with NEAT1 depletion proved less potent for the activation of mouse bone marrow cells than that of virus-infected cells without NEAT1 depletion (Figure 5F). As expected from this result, mouse bone marrow cells showed more activation in response to the supernatant of cells ectopically expressing mNeat1v2 than to the supernatant of control cells (Figure 5F). To strengthen this observation, we performed a similar experiment using immune cells. The chemotaxis of dimethylsulfoxide differentiated HL-60 (DMSO-HL60) cells, neutrophil-like cells, were more activated by the supernatant of virus-infected cells without NEAT1 depletion than by that of virus-infected cells depleted in NEAT1 (Figure 5G). DMSO-HL60 cells showed more activation in response to the supernatant of cells ectopically expressing mNeat1v2 than to the supernatant of control

(C) Schematic of the 5′ region of the *IL8* gene. Fine line, medium gray line, thick black line, and hatched line box indicate the promoter region, 5′ UTR, ORF, and SFPQ binding sequence, respectively. Gray lines below the *IL8* gene indicate the regions amplified by the qPCR primer sets for chromatin immunoprecipitation (ChIP) analysis. The panel at the bottom of the figure shows the conservation score of sequences along the 5′ region of the *IL8* gene. Transcriptional regulatory elements along this region are indicated.

(D) HeLa TO cells stimulated with (black bar) and without (white bar) poly I:C were subjected to ChIP of the 5′ region of the *IL8* gene. Error bars indicate the errors of two replicates.

(E) ChIP of the 5′ region of the *IL8* gene of HeLa TO cells transfected with either mock vector (white bar), pCMV-mNeat1v1 (gray bar), or pCMV-mNeat1v2 (black bar). Error bars indicate the errors of two replicates.

(F) The amount of NEAT1v2 coimmunoprecipitated with endogenous SFPQ was determined by RT-qPCR analysis. The relative amount of NEAT1v2 isolated by anti-SFPQ antibody was normalized to that isolated by the control IgG. Black and white bars indicate the relative amount of NEAT1v2 isolated from cells treated with or without poly I:C, respectively. Values represent the mean ± SD (*$p < 0.01$, Student's t test).

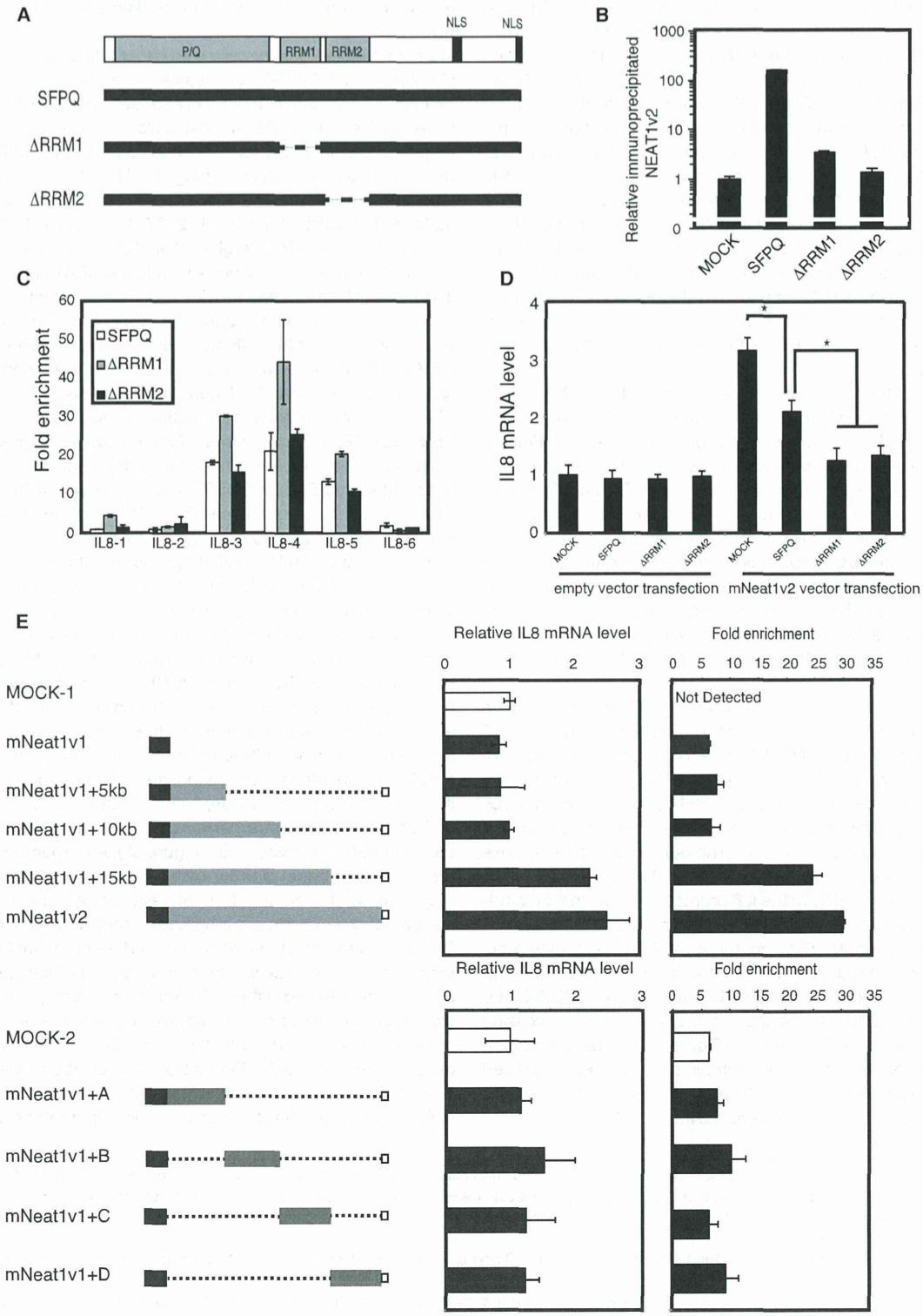

(legend on next page)

cells (Figure 5G). These results indicate that NEAT1 is induced by certain viruses and that it plays an important role in the innate immune response to viral infection.

DISCUSSION

In this study, we report that NEAT1 is induced by viral infection as well as by poly I:C stimulation. Moreover, we found that the stimulus-responsive cooperative action of NEAT1 and SFPQ regulates the expression of genes including those of antiviral factors such as cytokines (Figure 6).

The mechanisms of action of lncRNAs are diverse, ranging from guidance of the chromatin-modifying complexes to acting as "molecular sponges" for the capture of microRNAs (Mercer et al., 2009; Wang and Chang, 2011). For example, lncRNA GAS5 interacts directly with the DNA-binding domain of the glucocorticoid receptor, preventing the receptor from binding to its DNA response element, thereby in effect acting as a molecular decoy (Kino et al., 2010; Tani et al., 2013). LncRNA MALAT1 and TUG1 promote the relocalization of growth-control genes between nuclear subcompartments and thereby regulate gene expression during growth signaling (Yang et al., 2011). More recently, Hirose et al. reported the role of NEAT1 in transcriptional regulation through the sequestering of SFPQ from the RNA-specific adenosine deaminase B2 (ADARB2) gene in response to proteasome inhibition (Hirose et al., 2014). In contrast to our result, the authors showed the importance of the NEAT1-SFPQ interaction in the reduction of ADARB2 transcription. Thus, the NEAT1-SFPQ interaction plays roles in both repression and activation of genes, likely depending on the context of the promoter sequence or interplay with other transcriptional factor(s).

Although there are increasing data that show that lncRNA-protein interactions appear to function in the regulation of gene expression patterns, the identification of the critical short RNA sequences in functional lncRNAs was limited. We attempted to determine the minimal short RNA region in NEAT1 with which SFPQ interacts. We extrapolated the SFPQ binding region in NEAT1v2 by employing the data set of a recent study that systematically identified the RNA sequence motifs recognized by SFPQ (Ray et al., 2013). The potential SFPQ binding sequences were identified in a broad region of NEAT1v2 (Figure S4A). Among these potential SFPQ binding sequences, we showed that two NEAT1 sequences, containing highly ranked SFPQ-binding RNA sequences reported by Ray et al., bound directly and specifically to SFPQ (Figures S4B–S4D). These SFPQ-binding NEAT1 RNAs did not affect the level of mNeat1v2-mediated IL8 transcription (Figure S4E), corresponding to the result in Figure 4. It has been reported that certain RNA binding proteins require a long length of the RNA binding partner to achieve adequate protein function. For instance, polycomb repressive complex 2 (PRC2), containing an RNA binding protein, shows higher affinity to longer partner lncRNAs (Davidovich et al., 2013). In a similar manner as PRC2, SFPQ may require a long NEAT1 RNA sequence (~15 kb) to exert proper function, namely releasing from the IL8 promoter as described in this research.

In this report, we focused on the role of NEAT1 in host antiviral response. However, NEAT1 is also likely to regulate the expression of viral genes themselves, because several paraspeckle proteins are known to play a role in viral replication or viral gene expression (Oakland et al., 2013; Zhang et al., 2008; Zolotukhin et al., 2003). It is reasonable to assume that NEAT1-mediated remodeling of the nuclear localization of paraspeckle proteins directly affects viral replication and/or viral gene expression. Indeed, a recent report observed that NEAT1 modulates HIV-I replication by affecting the nucleus-to-cytoplasm export of Rev-dependent instability element-containing HIV-I mRNAs (Zhang et al., 2013). They showed that MALAT1 lncRNA localized in nuclear speckles was also induced by HIV infection. However, MALAT1 was not induced by poly I:C treatment and virus infections (Figure S5I). Thus, the induction of NEAT1 in response to viral infection may be a more general phenomenon than MALAT1 induction. In the present work, we propose that the TLR3-p38 pathway contributes to the induction of NEAT1 in response to poly I:C stimulation. Since poly I:C generally simulates the action of dsRNAs produced by viral infection, we speculate that viral infections also induce NEAT1 through the TLR3-p38 pathway. Analysis of the paraspeckle entities will reveal a novel mode(s) of viral replication and will contribute to a deeper understanding of viral life cycles and to the development of antiviral drugs.

The transcriptional regulation of cytokine genes in response to pathogen infection lies at the heart of immune response research. In terms of the transcriptional activation of the *IL8* gene, NF-κB, AP-1, and C/EBP play an important role. In this report, we have added another layer to knowledge of the transcriptional regulation system by uncovering the cooperative action between nuclear lncRNA and transcriptional regulator. The

Figure 4. Structure-Function Relationship Study of SFPQ and NEAT1

(A) Schematic diagrams of SFPQ deletion mutants. P/Q, RRM, and NLS indicate the P/Q domain, RNA binding motif, and nuclear localization signal, respectively. Dashed lines indicate the deleted regions in the mutant SFPQs.

(B) RNA immunoprecipitation experiment of the SFPQs. Cells transfected with plasmids expressing FLAG-tagged SFPQs were subjected to immunoprecipitation using an anti-FLAG antibody (clone M2; Sigma). The amounts of NEAT1v2 coimmunoprecipitated with the indicated FLAG-tagged SFPQs were determined by RT-qPCR analysis. The relative amounts of NEAT1v2 isolated by the anti-FLAG antibody were normalized to that isolated by the control IgG.

(C) ChIP analysis of the 5′ region of the *IL8* gene in HeLa TO cells transfected with plasmids expressing the indicated FLAG-tagged SFPQs. The relative amounts of IL8 promoter region DNA isolated by the anti-FLAG antibody were normalized to that isolated by the control IgG. Error bars indicate the errors of two replicate experiments.

(D) IL8 mRNA levels in HeLa TO cells transfected with plasmids expressing the indicated SFPQs in the presence or absence of mNeat1v2 expression. Values represent the mean ± SD (*$p < 0.01$, Student's t test).

(E) IL8 mRNA induction activity and SFPQ binding activity of mutant mNeat1s. Black and gray boxes indicate mNeat1v1 and mNeat1v2, respectively. Dashed lines indicate deleted regions. Schematic structures of the mNeat1v2 deletion mutants are indicated on the left. IL8 mRNA induction determined by RT-qPCR and SFPQ binding determined by RNA immunoprecipitation experiments are shown in the center and right, respectively.

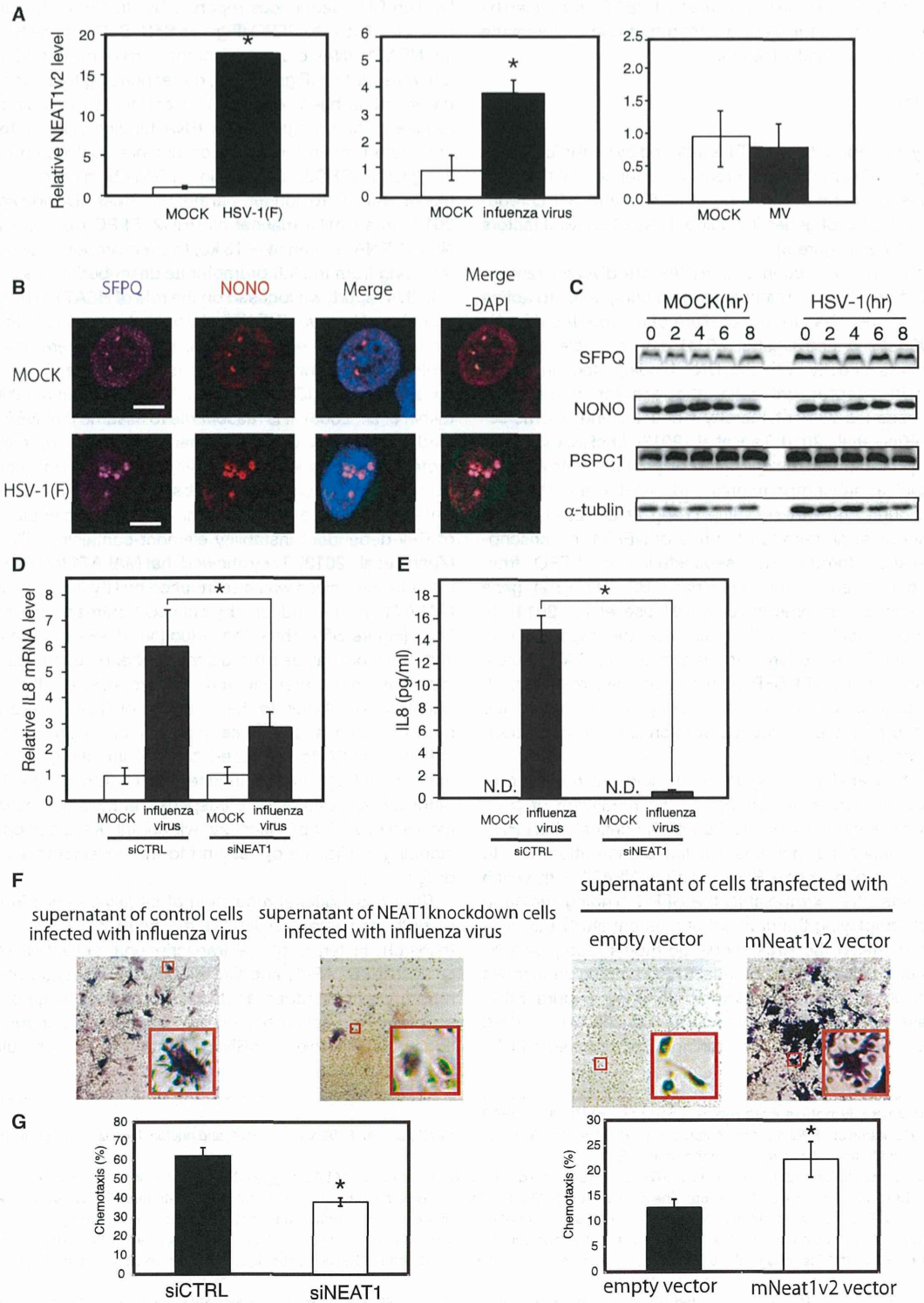

Figure 5. Effect of Viral Infection on NEAT1v2 Induction, Paraspeckle Formation, IL8 Induction, and the Activation of Bone Marrow Cells

(A) NEAT1v2 levels were quantified by RT-qPCR in cells infected with influenza virus, herpes simplex virus 1 (HSV-1), or measles virus (MV). The 18S ribosomal RNA level was used as a normalization control. Values represent the mean ± SD (*$p < 0.01$, Student's t test).

(legend continued on next page)

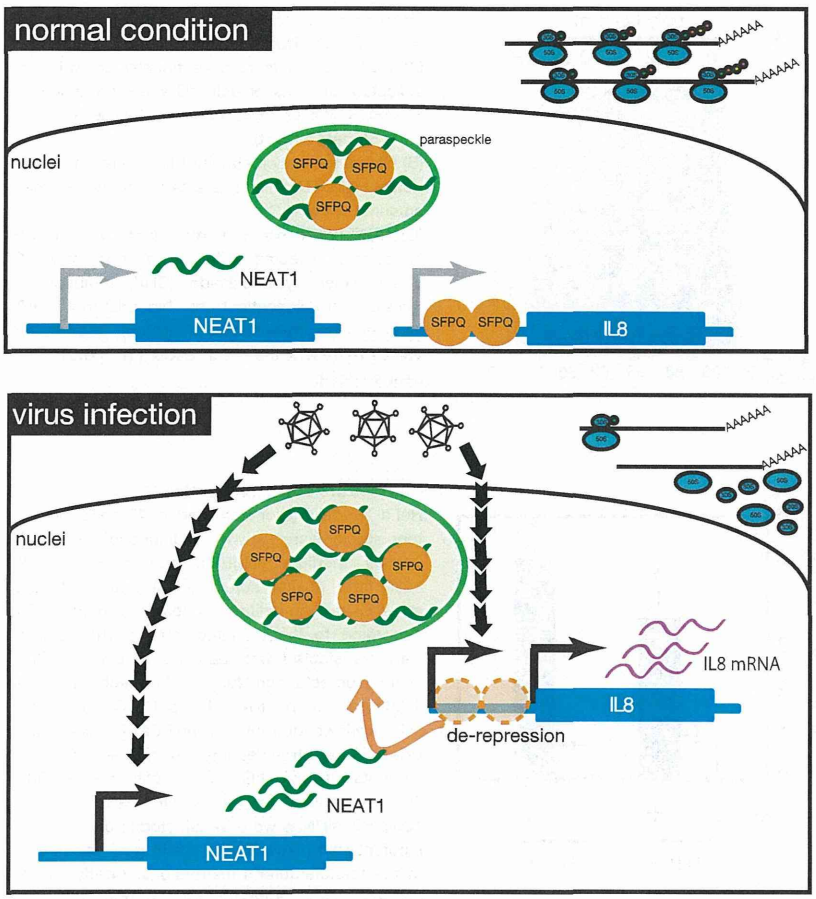

Figure 6. Model of the Transcriptional Regulation of Antiviral Genes Regulated by the Coordinated Action of NEAT1 and Paraspeckle Protein

SFPQs are both located in paraspeckles and bound to gene promoters such as *IL8* under normal conditions. Here, SFPQ represses the transcription of the *IL8* gene. Upon viral infection or poly I:C stimulation, NEAT1 is induced. In the case of poly I:C stimulation, NEAT1 is induced by the TLR3-p38 pathway. NEAT1 induction relocates SFPQ from the *IL8* promoter region and forms excess paraspeckles, consequently activating *IL8* transcription.

high evolutionary conservation of the SFPQ-binding sequence (Figure 3C and Table S3), comparable to that of the AP-1 and C/EBP sites, emphasizes the importance of SFPQ-mediated transcriptional regulation of the *IL8* gene. The established modes of transcriptional activation (NF-κB and so on) and the lncRNA-mediated mode of transcriptional regulation (this study) therefore work in synergy to achieve the precise transcriptional regulation of cytokine genes required during immune response.

SFPQ is known as a multifunctional protein involved in several vital cellular processes, such as pre-mRNA processing. We therefore examined whether NEAT1 controls the function of SFPQ in splicing. We surveyed genes whose splicing patterns were influenced by poly I:C treatment and restored by NEAT1 depletion through a massive sequencing analysis. The poly I:C-induced altered splicing of the *Serine palmitoyltransferase, long chain base subunit 1* gene (increase in variant NM_178324 from 20% to 33%) was restored by NEAT1 depletion (from 28% to 33%) (Figures S2J and S2K). Thus, NEAT1 is also involved in the regulation of SFPQ-mediated splicing regulation.

In this report, there are somewhat superficial nonlinear correlations among NEAT1 expression level, IL8 expression level, SFPQ localization, and paraspeckle size. We think that these superficial nonlinear correlations can be explained by the following interpretations. The *IL8* transcription is regulated by not only NEAT1-SFPQ cooperation, but also the NF-κB pathway. Since both poly I:C treatment and virus infection activate the NF-κB pathway, the effects of these stimuli for IL8 transcription are stronger than that of NEAT1 overexpression, which can only activate SFPQ-mediated IL8 transcription. Therefore, the elevated level of NEAT1v2 (causing excess formation of paraspeckles, but not inducing NF-κB activation) did not lead to a strong induction of IL8 mRNA expression compared with poly I:C treatment or viral infections. Another potential explanation is the presence of multiple functions in SFPQ. Several SFPQ-mediated gene regulation pathways might be involved in the upregulation of IL8 mRNA expression in response to SFPQ depletion. If SFPQ destabilized IL8 mRNA, depletion of SFPQ would increase IL8 mRNA through mRNA stabilization and transcriptional activation. If this was the

(B) HeLa TO cells infected with HSV-1 were subjected to visualization of SFPQ (magenta) and NONO (red) by immunostaining, and of the nuclei by staining with DAPI.
(C) The levels of paraspeckle proteins were analyzed by western blotting at various points post-HSV-1 infection.
(D and E) IL8 mRNA and protein levels were quantified by RT-qPCR and ELISA, respectively, in NEAT1 knockdown cells or control cells infected with (black bars) or without (white bars) influenza virus. Values represent the mean ± SD (*$p < 0.01$, Student's t test).
(F) Microscopic observation of mouse bone marrow cells treated with the supernatants of the indicated cultured cells. The cells were stained using a TRACP and ALP double-stain kit. The red color-stained cells show TRACP activity, indicating the osteoclast differentiation. The blue color-stained cells show ALP activity, indicating the osteoblast differentiation. Values represent the mean ± SD (*$p < 0.01$, Student's t test).
(G) Chemotaxis of DMSO-HL60 cells were assessed by transwell assay. Migrated cells were counted under microscopic observation. Chemotaxis values ((migrated cells / total cells) × 100) represent the means ± SD of three independent experiments. Statistically significant differences ($p < 0.01$) were determined by Student's t test.

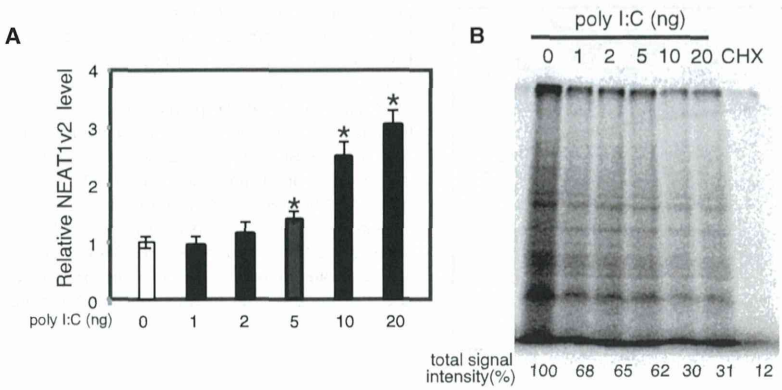

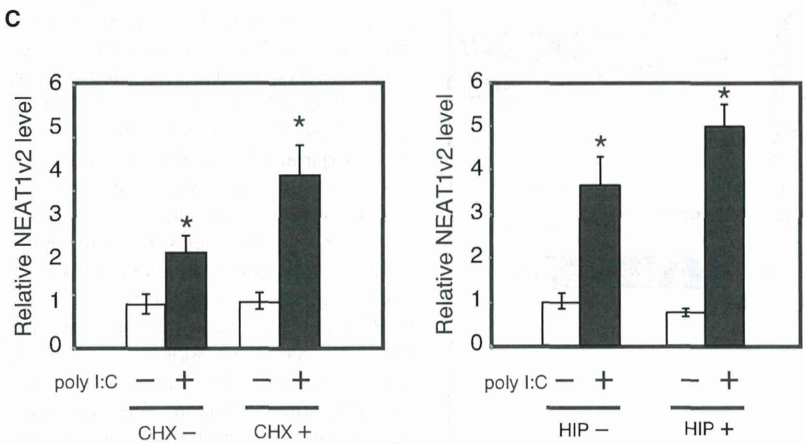

Figure 7. Induction of NEAT1v2 by Poly I:C under Translational Repression

(A) NEAT1v2 levels in cells transfected with the indicated amounts of poly I:C were quantified by RT-qPCR. Values represent the mean ± SD (*$p < 0.01$, Student's t test).

(B) Global translation status of transcription-incompetent HeLa TO cells transfected with the indicated amounts of poly I:C.

(C) NEAT1v2 levels were quantified by RT-qPCR in cells transfected with or without poly I:C under either cycloheximide (CHX; inhibitor for translational elongation) or hippuristanol (HIP; inhibitor for translational initiation) treatments. Values represent the mean ± SD (*$p < 0.01$, Student's t test).

case, depletion of SFPQ would have a stronger effect on the level of IL8 mRNA expression compared with NEAT1 induction-mediated SFPQ modulation. In addition, although NEAT1 should relocate SFPQ from the IL8 promoter, SFPQ proteins are still present in the nucleus. Such SFPQ, even enriched in paraspeckles, might have a certain effect on the IL8 mRNA expression level.

Translation in virus-infected cells is highly repressed (Sonenberg, 1990). For this reason, a translation-independent acute response system is necessary for early immune response. In this regard, the system proposed here is biologically meaningful, because NEAT1 is a noncoding RNA that exerts an effect without need for translation. Indeed, NEAT1 was induced in cells where translation was repressed by poly I:C stimulation (Figure 7). NEAT1v2 was also induced in cells treated with specific translation inhibitors (Figure 7). Translational inhibition did not affect the amounts of paraspeckle proteins (Figure S6B) or the formation of paraspeckles (Figure S6A). These results show that NEAT1v2 exerts an effect under translational repression. We therefore speculate that many other lncRNAs play a role in situations where translation is highly repressed, such as viral infection, heat shock, and hypoxia.

EXPERIMENTAL PROCEDURES

Reagents and Molecular Biological Products

All chemicals were purchased from Wako, unless otherwise stated.

Cell Culture and Transfection

HeLa TO cells (Clontech) and A549 cells (laboratory stock) were grown in Dulbecco's modified Eagle's medium (DMEM), supplemented with 10% fetal bovine serum (FBS) and antibiotics at 37°C in a humidified incubator with 5% CO_2. According to the manufacturer's protocol, cells were transfected with poly I:C or plasmid DNA using Lipofectamine 2000 or Lipofectamine LTX (Invitrogen), respectively. For poly I:C stimulation, cells were seeded into 12-well cell culture plates followed by transfection using the indicated amounts of poly I:C and Lipofectamine 2000. The sequences of the siRNAs are listed in Table S2. siRNAs were transfected into cells using Lipofectamine RNAiMAX (Invitrogen) according to the manufacturer's instructions. Briefly, siRNA duplexes (final concentration 10 nM) and cells were harvested 72 hr posttransfection. RT-qPCR was used to determine whether RNA interference achieved significant depletion of each target sequence.

ChIP Assay

Chromatin was crosslinked with 1% formaldehyde for 10 min at 37°C and then sonicated in lysis buffer (1% SDS, 10 mM EDTA, and 50 mM Tris [pH 8.0], plus protease inhibitor cocktail [Roche]). After centrifugation, 10 μl of the supernatant was used as input, and the remaining lysate was subjected to a ChIP assay using an anti-SFPQ mouse monoclonal antibody (clone B92, Sigma-Aldrich). The primers used to amplify the genes are listed in Table S1.

Viral Infection

HeLa TO cells were seeded into culture plates 1 day before infection and then infected with HSV-1(F) at a multiplicity of infection (moi) of 10. At 72 hr posttransfection with either siRNA or *mNeat1* cDNA, HeLa cells grown in DMEM supplemented with 10% FCS were infected with influenza A virus strain A/WSN/33 at a moi of 3. After incubation for 15 hr, the culture supernatants and total RNAs were collected and subjected to ELISA and RT-qPCR, respectively. MV (Edmonston strain) was propagated in Vero cells grown in DMEM supplemented with 2% FCS. A549 cells were infected with MV at a moi of 0.1.

SUPPLEMENTAL INFORMATION

Supplemental Information includes six figures, four tables, Supplemental Experimental Procedures, and two movies and can be found with this article online at http://dx.doi.org/10.1016/j.molcel.2014.01.009.

AUTHOR CONTRIBUTIONS

K.I., K.S., and N.A. conceived the research strategies, performed experiments, and wrote the paper. N.I., T. Yada, and Y.S. performed bioinformatics analyses. G.A. performed FISH and IF. T. Yamada and T.O. performed FRAP analysis and wrote the manuscript. M. Kumakura, A. Kawaguchi, K.N., A. Kato, Y.K., H.S., M.Y., and C.K. designed the virus infection experiments, performed experiments, and wrote the manuscript. T. Yada analyzed the SFPQ binding region and wrote the paper. K.K., K.I., M. Kobayashi, T.K., and Y.W. designed the microarray analysis, performed experiments, and wrote the manuscript.

ACKNOWLEDGMENTS

We thank Drs. T. Hirose (Hokkaido University) and S. Nakagawa (Riken) for providing mouse Neat1 expression vectors. We thank Drs. Y. Tomari (University of Tokyo), Y. Kumagai (Osaka University), Y.T. Sasaki (AIST), and Y. Hayashi (University of Tokyo) for fruitful discussion and critical comments. We also thank Dr. A. Fox (University of Western Australia), K. Lynch (University of Pennsylvania), A. Matsuzawa (University of Tokyo), and Y. Yoneyama (Chiba University) for providing the mouse monoclonal anti-NONO/p54 antibody, the HIS-SFPQ expression vector, anti-phospho-JNK antibody, and shRNA expression vector to silence RIG-I, respectively. This work was financially supported by the Suzuken Memorial Foundation, the Naito Foundation, Research Fellowship of the Japan Society for the Promotion of Science, Grant-in-Aid for Scientific Research (22310117, 23659050, 23790077), a Grant-in-Aid for Scientific Research on Innovative Areas "Functional machinery for noncoding RNAs," "Genome adaptation," and "Genome science" from the Ministry of Education, Culture, Sports, Science and Technology of Japan, and The Funding Program for World-Leading Innovative R&D on Science and Technology of the Japan Society for the Promotion of Science.

Received: June 6, 2013
Revised: November 8, 2013
Accepted: January 2, 2014
Published: February 6, 2014

REFERENCES

Arpaia, N., and Barton, G.M. (2011). Toll-like receptors: key players in antiviral immunity. Curr Opin Virol *1*, 447–454.

Berghäll, H., Sirén, J., Sarkar, D., Julkunen, I., Fisher, P.B., Vainionpää, R., and Matikainen, S. (2006). The interferon-inducible RNA helicase, mda-5, is involved in measles virus-induced expression of antiviral cytokines. Microbes Infect. *8*, 2138–2144.

Bernard, D., Prasanth, K.V., Tripathi, V., Colasse, S., Nakamura, T., Xuan, Z., Zhang, M.Q., Sedel, F., Jourdren, L., Coulpier, F., et al. (2010). A long nuclear-retained non-coding RNA regulates synaptogenesis by modulating gene expression. EMBO J. *29*, 3082–3093.

Carninci, P., Kasukawa, T., Katayama, S., Gough, J., Frith, M.C., Maeda, N., Oyama, R., Ravasi, T., Lenhard, B., Wells, C., et al.; FANTOM Consortium; RIKEN Genome Exploration Research Group and Genome Science Group (Genome Network Project Core Group) (2005). The transcriptional landscape of the mammalian genome. Science *309*, 1559–1563.

Chen, L.L., and Carmichael, G.G. (2009). Altered nuclear retention of mRNAs containing inverted repeats in human embryonic stem cells: functional role of a nuclear noncoding RNA. Mol. Cell *35*, 467–478.

Chen, L.L., and Carmichael, G.G. (2010). Decoding the function of nuclear long non-coding RNAs. Curr. Opin. Cell Biol. *22*, 357–364.

Clemson, C.M., Hutchinson, J.N., Sara, S.A., Ensminger, A.W., Fox, A.H., Chess, A., and Lawrence, J.B. (2009). An architectural role for a nuclear noncoding RNA: NEAT1 RNA is essential for the structure of paraspeckles. Mol. Cell *33*, 717–726.

Davidovich, C., Zheng, L., Goodrich, K.J., and Cech, T.R. (2013). Promiscuous RNA binding by Polycomb repressive complex 2. Nat. Struct. Mol. Biol. *20*, 1250–1257.

Fox, A.H., and Lamond, A.I. (2010). Paraspeckles. Cold Spring Harb. Perspect. Biol. *2*, a000687.

Guillot, L., Le Goffic, R., Bloch, S., Escriou, N., Akira, S., Chignard, M., and Si-Tahar, M. (2005). Involvement of toll-like receptor 3 in the immune response of lung epithelial cells to double-stranded RNA and influenza A virus. J. Biol. Chem. *280*, 5571–5580.

Gupta, R.A., Shah, N., Wang, K.C., Kim, J., Horlings, H.M., Wong, D.J., Tsai, M.C., Hung, T., Argani, P., Rinn, J.L., et al. (2010). Long non-coding RNA HOTAIR reprograms chromatin state to promote cancer metastasis. Nature *464*, 1071–1076.

Guttman, M., Amit, I., Garber, M., French, C., Lin, M.F., Feldser, D., Huarte, M., Zuk, O., Carey, B.W., Cassady, J.P., et al. (2009). Chromatin signature reveals over a thousand highly conserved large non-coding RNAs in mammals. Nature *458*, 223–227.

Hirose, T., Virnicchi, G., Tanigawa, A., Naganuma, T., Li, R., Kimura, H., Yokoi, T., Nakagawa, S., Bénard, M., Fox, A.H., and Pierron, G. (2014). NEAT1 long noncoding RNA regulates transcription via protein sequestration within subnuclear bodies. Mol. Biol. Cell *25*, 169–183.

Hoffmann, E., Dittrich-Breiholz, O., Holtmann, H., and Kracht, M. (2002). Multiple control of interleukin-8 gene expression. J. Leukoc. Biol. *72*, 847–855.

Huarte, M., and Rinn, J.L. (2010). Large non-coding RNAs: missing links in cancer? Hum. Mol. Genet. *19* (R2), R152–R161.

Hutchinson, J.N., Ensminger, A.W., Clemson, C.M., Lynch, C.R., Lawrence, J.B., and Chess, A. (2007). A screen for nuclear transcripts identifies two linked noncoding RNAs associated with SC35 splicing domains. BMC Genomics *8*, 39.

Iacobazzi, V., Infantino, V., Costanzo, P., Izzo, P., and Palmieri, F. (2005). Functional analysis of the promoter of the mitochondrial phosphate carrier human gene: identification of activator and repressor elements and their transcription factors. Biochem. J. *391*, 613–621.

Kapranov, P., Willingham, A.T., and Gingeras, T.R. (2007). Genome-wide transcription and the implications for genomic organization. Nat. Rev. Genet. *8*, 413–423.

Kawai, T., and Akira, S. (2010). The role of pattern-recognition receptors in innate immunity: update on Toll-like receptors. Nat. Immunol. *11*, 373–384.

Kino, T., Hurt, D.E., Ichijo, T., Nader, N., and Chrousos, G.P. (2010). Noncoding RNA gas5 is a growth arrest- and starvation-associated repressor of the glucocorticoid receptor. Sci. Signal. *3*, ra8.

Koide, M., Kinugawa, S., Takahashi, N., and Udagawa, N. (2010). Osteoclastic bone resorption induced by innate immune responses. Periodontol. 2000 *54*, 235–246.

Lafaille, F.G., Pessach, I.M., Zhang, S.Y., Ciancanelli, M.J., Herman, M., Abhyankar, A., Ying, S.W., Keros, S., Goldstein, P.A., Mostoslavsky, G., et al. (2012). Impaired intrinsic immunity to HSV-1 in human iPSC-derived TLR3-deficient CNS cells. Nature *491*, 769–773.

Mao, Y.S., Zhang, B., and Spector, D.L. (2011). Biogenesis and function of nuclear bodies. Trends Genet. *27*, 295–306.

Mercer, T.R., Dinger, M.E., and Mattick, J.S. (2009). Long non-coding RNAs: insights into functions. Nat. Rev. Genet. *10*, 155–159.

Miyagawa, R., Tano, K., Mizuno, R., Nakamura, Y., Ijiri, K., Rakwal, R., Shibato, J., Masuo, Y., Mayeda, A., Hirose, T., and Akimitsu, N. (2012). Identification of cis- and trans-acting factors involved in the localization of MALAT-1 noncoding RNA to nuclear speckles. RNA *18*, 738–751.

Mizutani, R., Wakamatsu, A., Tanaka, N., Yoshida, H., Tochigi, N., Suzuki, Y., Oonishi, T., Tani, H., Tano, K., Ijiri, K., et al. (2012). Identification and characterization of novel genotoxic stress-inducible nuclear long noncoding RNAs in mammalian cells. PLoS ONE *7*, e34949.

Naganuma, T., and Hirose, T. (2013). Paraspeckle formation during the biogenesis of long non-coding RNAs. RNA Biol. *10*, 456–461.

Naganuma, T., Nakagawa, S., Tanigawa, A., Sasaki, Y.F., Goshima, N., and Hirose, T. (2012). Alternative 3′-end processing of long noncoding RNA initiates construction of nuclear paraspeckles. EMBO J. *31*, 4020–4034.

Nakagawa, S., and Hirose, T. (2012). Paraspeckle nuclear bodies—useful uselessness? Cell. Mol. Life Sci. *69*, 3027–3036.

Oakland, T.E., Haselton, K.J., and Randall, G. (2013). EWSR1 binds the hepatitis C virus cis-acting replication element and is required for efficient viral replication. J. Virol. *87*, 6625–6634.

Peng, R., Dye, B.T., Pérez, I., Barnard, D.C., Thompson, A.B., and Patton, J.G. (2002). PSF and p54nrb bind a conserved stem in U5 snRNA. RNA *8*, 1334–1347.

Ponting, C.P., Oliver, P.L., and Reik, W. (2009). Evolution and functions of long noncoding RNAs. Cell *136*, 629–641.

Prasanth, K.V., and Spector, D.L. (2007). Eukaryotic regulatory RNAs: an answer to the 'genome complexity' conundrum. Genes Dev. *21*, 11–42.

Rathinam, V.A., and Fitzgerald, K.A. (2011). Cytosolic surveillance and antiviral immunity. Curr Opin Virol *1*, 455–462.

Ray, D., Kazan, H., Cook, K.B., Weirauch, M.T., Najafabadi, H.S., Li, X., Gueroussov, S., Albu, M., Zheng, H., Yang, A., et al. (2013). A compendium of RNA-binding motifs for decoding gene regulation. Nature *499*, 172–177.

Saha, S., Murthy, S., and Rangarajan, P.N. (2006). Identification and characterization of a virus-inducible non-coding RNA in mouse brain. J. Gen. Virol. *87*, 1991–1995.

Sasaki, Y.T., Ideue, T., Sano, M., Mituyama, T., and Hirose, T. (2009). MENepsilon/beta noncoding RNAs are essential for structural integrity of nuclear paraspeckles. Proc. Natl. Acad. Sci. USA *106*, 2525–2530.

Scaria, V., and Pasha, A. (2012). Long Non-Coding RNAs in Infection Biology. Front Genet *3*, 308.

Sonenberg, N. (1990). Measures and countermeasures in the modulation of initiation factor activities by viruses. New Biol. *2*, 402–409.

Song, X., Sui, A., and Garen, A. (2004). Binding of mouse VL30 retrotransposon RNA to PSF protein induces genes repressed by PSF: effects on steroidogenesis and oncogenesis. Proc. Natl. Acad. Sci. USA *101*, 621–626.

Sunwoo, H., Dinger, M.E., Wilusz, J.E., Amaral, P.P., Mattick, J.S., and Spector, D.L. (2009). MEN epsilon/beta nuclear-retained non-coding RNAs are up-regulated upon muscle differentiation and are essential components of paraspeckles. Genome Res. *19*, 347–359.

Tani, H., Mizutani, R., Salam, K.A., Tano, K., Ijiri, K., Wakamatsu, A., Isogai, T., Suzuki, Y., and Akimitsu, N. (2012). Genome-wide determination of RNA stability reveals hundreds of short-lived noncoding transcripts in mammals. Genome Res. *22*, 947–956.

Tani, H., Torimura, M., and Akimitsu, N. (2013). The RNA degradation pathway regulates the function of GAS5 a non-coding RNA in mammalian cells. PLoS ONE *8*, e55684.

Tano, K., Mizuno, R., Okada, T., Rakwal, R., Shibato, J., Masuo, Y., Ijiri, K., and Akimitsu, N. (2010). MALAT-1 enhances cell motility of lung adenocarcinoma cells by influencing the expression of motility-related genes. FEBS Lett. *584*, 4575–4580.

Thompson, M.R., Kaminski, J.J., Kurt-Jones, E.A., and Fitzgerald, K.A. (2011). Pattern recognition receptors and the innate immune response to viral infection. Viruses *3*, 920–940.

Urban, R.J., Bodenburg, Y., Kurosky, A., Wood, T.G., and Gasic, S. (2000). Polypyrimidine tract-binding protein-associated splicing factor is a negative regulator of transcriptional activity of the porcine p450scc insulin-like growth factor response element. Mol. Endocrinol. *14*, 774–782.

Wang, K.C., and Chang, H.Y. (2011). Molecular mechanisms of long noncoding RNAs. Mol. Cell *43*, 904–914.

Yang, L., Lin, C., Liu, W., Zhang, J., Ohgi, K.A., Grinstein, J.D., Dorrestein, P.C., and Rosenfeld, M.G. (2011). ncRNA- and Pc2 methylation-dependent gene relocation between nuclear structures mediates gene activation programs. Cell *147*, 773–788.

Yoon, J.H., Abdelmohsen, K., and Gorospe, M. (2013). Posttranscriptional Gene Regulation by Long Noncoding RNA. J. Mol. Biol. *425*, 3723–3730.

Zhang, S.Y., Jouanguy, E., Ugolini, S., Smahi, A., Elain, G., Romero, P., Segal, D., Sancho-Shimizu, V., Lorenzo, L., Puel, A., et al. (2007). TLR3 deficiency in patients with herpes simplex encephalitis. Science *317*, 1522–1527.

Zhang, W., Zhang, X., Tian, C., Wang, T., Sarkis, P.T., Fang, Y., Zheng, S., Yu, X.F., and Xu, R. (2008). Cytidine deaminase APOBEC3B interacts with heterogeneous nuclear ribonucleoprotein K and suppresses hepatitis B virus expression. Cell. Microbiol. *10*, 112–121.

Zhang, Q., Chen, C.Y., Yedavalli, V.S., and Jeang, K.T. (2013). NEAT1 long noncoding RNA and paraspeckle bodies modulate HIV-1 posttranscriptional expression. MBio *4*, e00596–e12.

Zolotukhin, A.S., Michalowski, D., Bear, J., Smulevitch, S.V., Traish, A.M., Peng, R., Patton, J., Shatsky, I.N., and Felber, B.K. (2003). PSF acts through the human immunodeficiency virus type 1 mRNA instability elements to regulate virus expression. Mol. Cell. Biol. *23*, 6618–6630.

FULL PAPER *Virology*

Construction of an Expression System for Bioactive IL-18 and Generation of Recombinant Canine Distemper Virus Expressing IL-18

Yuxiu LIU[1,2], Hiroki SATO[1]*, Masahiro HAMANA[1], Navita Anisia MOONAN[1], Misako YONEDA[1], Xianzhu XIA[2] and Chieko KAI[1]

[1]*Laboratory Animal Research Center, Institute of Medical Science, The University of Tokyo, 4–6–1 Shirokanedai, Minato-ku, Tokyo 108–8639, Japan*
[2]*College of Veterinary Medicine, Agricultural Division, Jilin University, Changchun 130062, China*

(Received 4 April 2014/Accepted 22 May 2014/Published online in J-STAGE 4 June 2014)

ABSTRACT. Interleukin 18 (IL-18) plays an important role in the T-helper-cell type 1 immune response against intracellular parasites, bacteria and viral infections. It has been widely used as an adjuvant for vaccines and as an anticancer agent. However, IL-18 protein lacks a typical signal sequence and requires cleavage into its mature active form by caspase 1. In this study, we constructed mammalian expression vectors carrying cDNA encoding mature canine IL-18 (cIL-18) or mouse IL-18 (mIL-18) fused to the human IL-2 (hIL-2) signal sequence. The expressed proIL-18 proteins were processed to their mature forms in the cells. The supernatants of cells transfected with these plasmids induced high interferon-γ production in canine peripheral blood mononuclear cells or mouse splenocytes, respectively, indicating the secretion of bioactive IL-18. Using reverse genetics, we also generated a recombinant canine distemper virus that expresses cIL-18 or mIL-18 fused to the hIL-2 signal sequence. As expected, both recombinant viruses produced mature IL-18 in the infected cells, which secreted bioactive IL-18. These results indicate that the signal sequence from hIL-2 is suitable for the secretion of mature IL-18. These recombinant viruses can also potentially be used as immunoadjuvants and agents for anticancer therapies *in vivo*.
KEY WORDS: canine distemper virus, interferon-γ, interleukin 18

doi: 10.1292/jvms.14-0181; *J. Vet. Med. Sci.* 76(9): 1241–1248, 2014

Canine distemper virus (CDV) is an enveloped, negative-sense, single-stranded RNA virus of the genus *Morbillivirus* in the family *Paramyxoviridae*, which causes a highly contagious and fatal multisystemic infection in domestic and wild carnivores [26]. CDV has ideal features for a live vaccine, because it not only induces an innate immune response, but also induces an adaptive immune response, which elicits life-long immunity in animals. In the 1950s, live attenuated CDV vaccines were introduced to prevent and reduce the incidence of canine distemper (CD) in susceptible animals. However, severe clinical CD outbreaks in immunized dogs have recently been documented [4, 16, 21]. Therefore, it is very important to improve the effects of the current vaccine. The production of highly neutralizing antibodies has always been used as a substitute marker to evaluate the immunogenicity and protective capacity of CDV vaccines, however, the induction of cell-mediated immunity has also been shown to be important for successful vaccination [1, 11, 15, 31].

IFN-γ is an important activator of macrophages and is critical for innate and adaptive immunity against viral and intracellular bacterial infections and for tumor control. IFN-γ is produced by NK cells and by natural killer T cells, $CD4^+$ Th1 cells and $CD8^+$ cytotoxic T lymphocytes, once antigen-specific immunity develops [33]. IL-12 and IL-18 are potent activators of IFN-γ production in NK and T cells and promote the development of T-helper type 1 responses [8, 39]. IL-12 has been extensively tested for its adjuvant activity. Increasing the dose of recombinant human IL-12 in a human cytomegalovirus (CMV) vaccine increased the anti-CMV gB IgG titer and CMV-specific $CD4^+$ T-cell proliferation [17]. DNA expressing IL-12 has also been shown to be an effective adjuvant for the simian immunodeficiency virus gag pDNA vaccine in rhesus macaques [32]. However, IL-12 is encoded by 2 separate genes, *IL12A*(p35) and *IL12B*(p40), requiring it to be cloned and expressed as 2 separate subunits in an *in vitro* study. It has been reported that IL-18 can also augment the IFN-γ-inducing capacity and antitumor activity independently of IL-12 [12]. To date, IL-18 has been used as a vaccine adjuvant and enhanced vaccine efficiency in mouse, cats, pigs and other mammals [20, 25, 28].

IL-18 is synthesized as a biologically inactive precursor protein (proIL-18, 22 kDa) by cells of the immune system and other types of cells [12]. ProIL-18 lacks a typical signal sequence for secretion [27] and is processed into its mature active form (mature IL-18, 18 kDa) by caspase-1 cleavage. Without the caspase-1 cleavage process, the mature IL-18 protein cannot be efficiently secreted across the cell membrane. Several reports have indicated that the addition of a signal sequence derived from various secreted proteins enhances the extracellular secretion of bioactive IL-18 [14, 24, 29]. It has been reported that the fusion of the canine IL12-p40 signal sequence (cIL-12p40ss) to mature canine IL-18 (cIL-18) enhanced the secretion efficiency of bioac-

*CORRESPONDENCE TO: SATO, H., Laboratory Animal Research Center, Institute of Medical Science, The University of Tokyo, 4–6–1 Shirokanedai, Minato-ku, Tokyo 108–8639, Japan.
e-mail: satohi@ims.u-tokyo.ac.jp

Table 1. Primers used for PCR amplification

Name	Primer sequences
*Sac*I-cIL18 F	5′-GAGCTCATGGCTGCTAACCTAATAGAAG-3
*Sac*I-cIL18 R	5′-GAGCTCATAGAACGGTTGGTCGGATG-3′
*Afl*II-cIL12p40 F	5′-CCTTAAGATGCATCCTCAGCAGTTGGTCATCTCC-3′
*Kpn*I-cIL12p40 R	5′-GGGTACCCTAACTGCAGGACACAGATGCCCAGTC-3′
*Nde*I-mature-cIL18 F	5′-GCATATGGTACTTTGGCAAGCTTGAACCTAAAC-3′
*Kpn*I-mature-cIL18 R	5′-GGTACCCTAGCTCTTGTTTTGAACAGTGAAC-3′
*Nco*I-mature-cIL18 F	5′-CCATGGCCTACTTTGGCAAGCTTGAACCTAAAC-3′
*Bgl*II-mature-cIL18 R	5′-AGATCTCTAGCTCTTGTTTTGAACAGTGAAC-3′
*Nco*I-mature-mIL18 F	5′-ATAGCCATGGCTAACTTTGGCCGACTTCAC-3′
*Bgl*II-mature-mIL18 R	5′-GGGGAGATCTCTAACTTTGATGTAAGTTAGTG-3′
*Fse*I-cIL18-CDV F	5′-GGCCGGCCaaactcattataaaaaacttagggctcaggtagtccaacaATGGCTGCTAACCTAATAGAAG-3′
*Fse*I-cIL18-CDV R	5′-GGCCGGCCTCTACTAGCTCTTGTTTTGAACAGTG-3′
*Fse*I-hIL2ss-CDV F	5′-GGCCGGCCTCTaaactcattataaaaaacttagggctcaggtagtccaacaATGTACAGGATGCAACTCCT-3′
*Fse*I-hIL2ss-cIL18-CDV R	5′-GGCCGGCCCTAGCTCTTGTTTTGAACAGTGAAC-3′
*Fse*I-hIL2ss-mIL18-CDV R	5′-GGCCGGCCCTAACTTTGATGTAAGTTAGTG-3′
CDV-N F	5′-TGGTTGGTGATCCGAAAATCAACGGACC-3′
CDV-N R	5′-CCCTCCCATGGAGTTTTCAAGTTCAACACC-3′

Restriction sites are underlined. CDV transcription signal unit sequences are described in lowercase letters.

tive IL-18 [37].

In the present study, we compared the secretion efficiency of signal sequence for bioactive cIL-18. We also generated a recombinant CDV (*r*CDV) expressing mature IL-18 as a new potential candidate vaccine adjuvant or anticancer reagent [34]. Interestingly, a recent study demonstrated that *r*CDV expressing rabies virus (RABV) G protein (RV-G) protected both dogs and mice against RABV challenge [39], even though mice are not a susceptible natural host of CDV. Therefore, we also tested mouse IL-18 in a similar manner.

MATERIALS AND METHODS

Cells and viruses: B95a (marmoset lymphoblastoid) cells [19] were maintained in RPMI 1640 medium (Gibco, Carlsbad, CA, U.S.A.), and HEK293 and 293T cells were cultured in Dulbecco's modified Eagle's medium (Sigma, St. Louis, MO, U.S.A.) supplemented with 5% FCS (Sigma), 100 U/m*l* penicillin G and 100 μg/m*l* streptomycin (Invitrogen, Carlsbd, CA, U.S.A.). The Yanaka strain of CDV [10] and the *r*CDVs were cultured with B95a cells in RPMI 1640 medium supplemented with 2% FCS. Canine PBMCs were isolated with Ficoll–Paque Plus (GE Healthcare, Amersham, U.K.), according to the manufacturer's instructions, from freshly drawn venous blood anticoagulated with 0.2 M EDTA, and maintained in RPMI 1640 medium supplemented with 10% FCS. Mouse spleen cells were prepared with a standard method and were cultured in RPMI 1640 medium supplemented with 10% FCS.

Mammalian expression plasmids: Canine PBMCs and mouse splenocytes were lysed with Isogen reagent (Nippon Gene, Tokyo, Japan) for RNA extraction, and the total RNAs isolated were reverse transcribed with SuperScript II Reverse Transcriptase (Invitrogen) and a random 6-mer primer. To construct a mammalian expression plasmid encoding the entire cIL-18, the full-length cIL-18 cDNA was amplified by PCR using canine PBMC cDNA, LA-Taq DNA polymerase (TaKaRa, Otsu, Japan) and a primer pair with *Sac*I restriction sites (*Sac*I-cIL18 F and *Sac*I-cIL18 R, Table 1). This was then inserted into the pCAGGS mammalian expression vector to generate pCAG–cIL18. To construct a mammalian expression plasmid encoding mature cIL-18 fused to the cIL12-p40 signal sequence, the cIL12-p40 cDNA was amplified by PCR from canine PBMC cDNA with a primer pair with *Afl*II and *Kpn*I restriction sites (*Afl*II-cIL12p40 F and *Kpn*I-cIL12p40 R, Table 1) and inserted into the pCAGGS vector, generating pCAG–cIL12p40. The cDNA of mature cIL-18, encoding amino acids 37–193, was amplified by PCR using a primer pair with *Nde*I and *Kpn*I restriction sites (*Nde*I-mature-cIL18F and *Kpn*I-mature-cIL18R, Table 1). pCAG–cIL12p40 was digested with *Nde*I immediately downstream from the cIL12-p40 signal sequence, and with *Kpn*I, and then introduced the mature cIL-18 cDNA digested with *Nde*I and *Kpn*I, generating pCAG–cIL12ss–cIL18. To construct a mammalian expression plasmid encoding mature cIL-18 or mIL-18 fused to the human IL-2 signal sequence, cDNA encoding mature cIL-18 or mature mIL-18 (amino acids 36–192) was amplified by PCR using primer pairs with *Nco*I and *Bgl*II restriction sites: for cIL-18, *Nco*I-mature-cIL18 F and *Bgl*II-mature-cIL18 R; for mIL-18, *Nco*I-mature-mIL18 F and *Bgl*II-mature-mIL18 R (Table 1). The cDNAs were digested with *Nco*I and *Bgl*II and inserted into the restriction sites in the eukaryotic expression vector pFuse–hIgG2–Fc2 (InvivoGen, San Diego, CA, U.S.A.), which contains the hIL-2 signal sequence for the secretion of fused proteins, generating pFuse–hIL2ss–cIL18 and pFuse–hIL2ss–mIL18.

Generation of rabbit polyclonal antibody against cIL-18: The cDNA of cIL-18 was cloned into pET42 (b) *E. coli* expression vector (Novagen, Darmstadt, Germany) in frame with C-terminal of glutathione-s-transferase (GST) (pET42-cIL18). A 1-liter culture of *E. coli* (BL21 strain) transformed